QUANTITATIVE EPMA COMPOSITIONAL MAPPING OF LUNAR MARE BASALT BRECCIA NORTHWEST AFRICA 12384.

P. K. Carpenter[1], B. L. Jolliff[1], R.L. Korotev[1], J. H. Tepper[2], A. J. Irving[3], and T.M. Hahn, Jr.[1] Dept. of Earth and Planetary Sciences, Washington University, St. Louis, MO, USA (paulc@wustl.edu); [2]Dept. of Geology, University of Puget Sound, Tacoma, WA, USA; [3]Dept. of Earth & Space Sciences, University of Washington, Seattle, WA, USA.

Introduction: In a companion abstract we present an overview of lunar mare basalt breccia Northwest Africa (NWA) 12384 [1]. Backscattered-electron mosaic imaging and X-ray intensity mapping using an AlMgFe RBG map were used to identify 24 prominent clasts in NWA 12384 endcut EC-1 (Fig. 1). Basalt clast 2, the largest in EC-1, is a pigeonite basalt containing: olivine, pigeonite with augite rims, intersertal ferroaugite, plagioclase, and a glass vein. We present detailed analysis of basalt clast 2 using EPMA spot analyses and quantitative compositional mapping to characterize the mineral chemistry, reconstruct the bulk composition, and discuss the results within the framework of lunar basalt petrology.

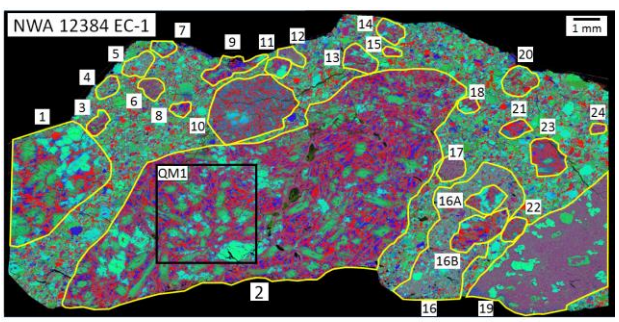

Figure 1 *AlMgFe RGB X-ray map of NWA 12384 with clast outlines and location of quantitative compositional map QM1 in basalt clast 2*.

EPMA Imaging and Quantitative Compositional Mapping: Region QM1 in basalt clast 2 was selected for quantitative map analysis (Fig. 1 and 2). We extend methods for compositional mapping established previously [2-5]. The JEOL JXA-8200 electron microprobe at Washington University was used with Probe for EPMA [6] to measure by wavelength-dispersive spectrometry, the elements Na, Mg, Al, Si, P, K, Ca, Ti, Cr, Mn, Fe, Ni, and Zr. WDS background correction was made using the mean atomic number (MAN) calibration, with full $\Phi(\rho z)$ correction relative to natural and synthetic mineral standards. Probe Image was used to acquire WDS stage maps of 1024 x 1024 pixels at 5 μm pixel size, using 100 nA probe current and 30 msec dwell time; 3 passes were used to measure the full element list. These digital X-ray intensity maps were converted to concentration units using CalcImage and Probe for EPMA, resulting in a complete analysis at each pixel. The resulting master data file (1,048,576 analyses) was used to generate element wt% images, which were input for kmeans unsupervised cluster analysis using the Fiji Xlib plugin [7]. The clusters define the average compositions and diversity of olivine, pyroxene, plagioclase, accessory phases, and glass from map QM1. Mineral data files for olivine, pyroxene, and plagioclase were generated from the master file based on stoichiometric relations, then filtered to select analytical totals of 99-101 wt% and appropriate cation sums so that the best analyses were used for plotting and interpretation.

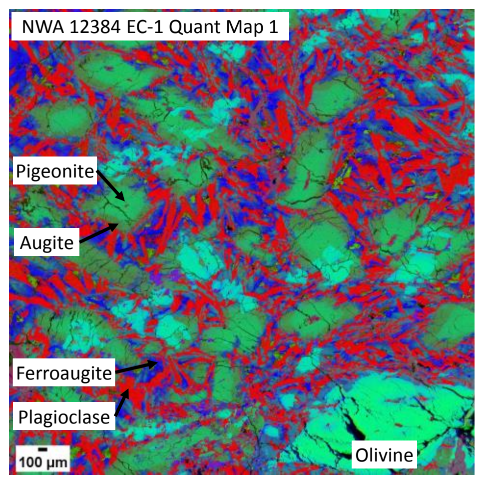

Figure 2. *Quantitative compositional map locator QM1 using AlMgFe composite X-ray maps. Olivine is blue-green, pigeonite green, augite rims dark green, ferroaugite blue, and plagioclase red*.

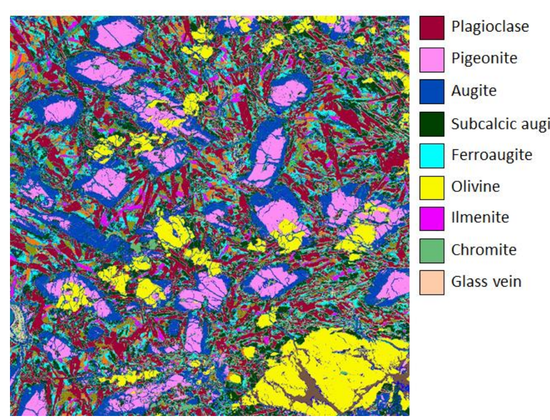

Figure 3. *Cluster classification map for QM1*.

Discussion: The results of the cluster analysis are an index map encoded for the identified clusters, the average and standard deviation of the cluster means, and the number of pixels assigned to the clusters. The index map is shown in Fig. 3, and the cluster compositions are listed in Table 1. The mineral compositions for plagioclase and pyroxene from the filtered data sets are shown in Fig. 4, along with the pyroxene clusters for comparison. The equivalent stoichiometry and endmember components for these clusters are:

Plagioclase $Ca_{0.80}Na_{0.14}K_{0.01}Al_{1.65}Si_{2.25}O_8$ sum 4.99 $An_{83.8}Or_{1.1}$
Pigeonite $Ca_{0.22}Mg_{1.13}Fe_{0.58}Al_{0.09}Si_{1.92}O_6$ sum 4.00, $Fs_{30.0}Wo_{11.2}$
Augite $Ca_{0.59}Mg_{0.79}Fe_{0.49}Al_{0.17}Si_{1.87}O_6$ sum 4.00, $Fs_{26.3}Wo_{31.6}$
Subcalcic augite
$Ca_{0.32}Mg_{0.74}Fe_{0.85}Al_{0.12}Si_{1.90}O_6$ sum 4.00, $Fs_{44.5}Wo_{16.7}$
Ferroaugite
$Ca_{0.53}Mg_{0.38}Fe_{0.99}Al_{0.12}Si_{1.89}O_6$ sum 3.99, $Fs_{52.2}Wo_{27.9}$
Olivine $Mg_{1.30}Fe_{0.66}Ca_{0.04}Si_{0.98}O_4$ sum 3.01, $Fa_{33.6}$

These cluster means have excellent stoichiometry and are equivalent to EPMA spot analyses. The wt% of each phase was calculated from the area fraction and appropriate phase density, then the summed contribution of each phase was used to reconstruct the bulk composition of clast 2. This composition is compared with the bulk composition of NWA 12384 determined by wet chemistry (Table 1), and are very similar considering that clast 2 is the dominant portion of EC-1. However, basalt clast 2 is lower in Mg and higher in Al, Ti, and Cr, compared to the more mafic bulk composition of NWA 12384. The bulk compositions differ from the EPMA spot analyses of the EC-1 glass vein, particularly for Ti, Al, Fe, and Mg. The composition of glass veins reflects the source lithology and degree of melting, which likely differs from the bulk composition. In summary, the quantitative compositional mapping methods we have developed have been used to accurately calculate the mineral and bulk composition of clast 2, and demonstrate a valuable analytical tool for the interpretation of lunar samples.

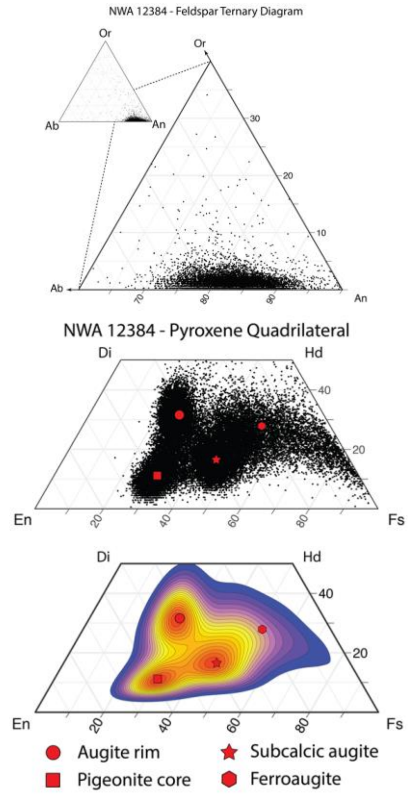

Figure 4 *Compositional variation exhibited by plagioclase (top, n=11077) and pyroxene (bottom, n=33855), using filtered data from QM1 quantitative map. Cluster mean compositions plotted for comparison.*

	Plagio clase	Pigeo nite	Augite	Subcalcic augite	Ferro augite	Olivine	Ilmenite	Bulk Recalc.	Bulk WC	Glass vein
SiO_2	49.61	51.93	48.46	48.85	45.77	36.56	8.02	45.60	45.25	45.94
TiO_2	0.24	0.72	1.47	1.51	1.68	0.11	44.81	2.70	2.00	3.47
Al_2O_3	31.02	2.04	4.31	2.84	2.60	0.42	1.35	8.82	7.51	12.64
Cr_2O_3	0.01	0.75	0.69	0.32	0.18	0.31	0.22	0.55	0.30	0.25
FeO	1.93	18.44	15.47	25.37	30.41	28.49	39.70	20.32	20.43	18.46
MnO	0.02	0.33	0.27	0.38	0.40	0.29	0.31	0.27	0.28	0.23
MgO	0.64	19.97	12.82	12.01	6.41	30.86	1.30	11.32	13.98	6.02
CaO	16.18	5.41	14.46	7.93	12.46	0.93	2.80	9.70	9.81	10.48
Na_2O	1.64	0.05	0.18	0.08	0.08	0.02	0.13	0.40	0.40	0.61
K_2O	0.17	0.01	0.03	0.04	0.06	0.01	0.05	0.08	0.01	0.17
P_2O_5	0.05	0.00	0.05	0.03	0.24	0.02	0.18	0.09	0.13	0.21
Total	101.50	99.64	98.22	99.36	100.30	98.01	98.88	99.85	100.90	98.49
Wt% phase	18.56	12.40	14.71	17.50	9.91	11.53	3.54			
Mg#		0.66	0.62	0.47	0.28	0.66		0.50	0.55	0.37

Not including chromite, cluster glass vein, fayalite-hedenbergite, cracks, alteration, clusters representing phase boundaries
Number of analyses: plagioclase 204432, pigeonite 111147, augite 131099, subcalcic augite 151488, ferroaugite 85768, olivine 105864, ilmenite 22356, EPMA glass vein 10
Phase wt% example: plagioclase area fraction 0.2225, density 2.75, AF*D = 0.6118, bulk density 3.30, wt% = 100*0.6118/3.30 = 18.56

Table 1. *Cluster averages of mineral phases (plagioclase – ilmenite), reconstructed EPMA bulk composition (Bulk recalc.). Compare with bulk wet chemistry (Bulk WC), and average of 10 EPMA spot analyses of glass vein (Glass vein).*

References: [1] Carpenter P. et al. (2019) LPS **L** 2125; [2] Carpenter P. (2018) Microsc. Microanal. 24(1) 780-781; [3] Carpenter P. et al. (2017) LPS **XLVII** 2607; [4] Hahn T. et al. (2017) Microsc. Microanal. 23(1) 1068-1069; [5] Carpenter P. et al. (2017) Microsc. Microanal. 23(1) 1068-1069; [6] https://www.probesoftware.com/ [7] https://imagej.net/Xlib